

Segmental distribution and morphometric features of primary sensory neurons projecting to the tibial periosteum in the rat

Mariusz Gajda¹, Jan A. Litwin¹, Dirk Adriaensen², Jean-Pierre Timmermans²
and Tadeusz Cichocki¹

¹Department of Histology, Jagiellonian University Medical College, Cracow, Poland

²Laboratory of Cell Biology and Histology, University of Antwerp - RUCA, Antwerp, Belgium

Abstract: Previous reports have demonstrated very rich innervation pattern in the periosteum. Most of the periosteal fibers were found to be sensory in nature. The aim of this study was to identify the primary sensory neurons that innervate the tibial periosteum in the adult rat and to describe the morphometric features of their perikarya. To this end, an axonal fluorescent carbocyanine tracer, DiI, was injected into the periosteum on the medial surface of the tibia. The perikarya of the sensory fibers were traced back in the dorsal root ganglia (DRG) L1-L6 by means of fluorescent microscopy on cryosections. DiI-containing neurons were counted in each section and their segmental distribution was determined. Using PC-assisted image analysis system, the size and shape of the traced perikarya were analyzed. DiI-labeled sensory neurons innervating the periosteum of the tibia were located in the DRG ipsilateral to the injection site, with the highest distribution in L3 and L4 (57% and 23%, respectively). The majority of the traced neurons were of small size (area < 850 μm^2), which is consistent with the size distribution of CGRP- and SP-containing cells, regarded as primary sensory neurons responsible for perception of pain and temperature. A small proportion of labeled cells had large perikarya and probably supplied corpuscular sense receptors observed in the periosteum. No differences were found in the shape distribution of neurons belonging to different size classes.

Key words: Periosteum - Innervation - Dorsal root ganglion - DiI tracing - Rat

Introduction

The periosteum has been shown to be the most densely innervated tissue of the bone organ [18]. Early histological reports based on methylene blue staining and silver impregnation have demonstrated an intense periosteal innervation in different species including rats [30] and humans [21, 24]. These anatomical observations were later supplemented by immunohistochemical and denervation studies [9, 13]. The nerve fibers located in the periosteum predominantly accompany blood vessels and are either sensory or sympathetic in nature [4, 5, 13]. The majority of the periosteal fibers belongs to the afferent limb originating in primary sensory neurons of the corresponding dorsal root ganglia. Sensory fibers were found both in the superficial fibrous layer of the periosteum and in the deep cellular lining [8, 13]. Post-

natal capsaicin treatment resulted in a marked depletion of these periosteal sensory fibers [13, 14], in line with earlier reports showing the capsaicin sensitivity of the neurons present in spinal and trigeminal ganglia [22, 28]. Immunohistochemistry further revealed that a large proportion of the periosteal fibers is immunoreactive for substance P (SP) and calcitonin gene-related peptide (CGRP) [4, 13, 18]. These neurotransmitters are well known markers of thin sensory fibers predominantly involved in nociception. A significant increase in the expression of SP in these fibers was observed during osteoarthritis, an inflammatory process that also affects the neighbouring regions of the periosteum [17]. CGRP and SP are also the most frequent neuropeptides found in DRG neurons, where they constitute approximately 50% and 35% of primary sensory neurons, respectively, and show a considerable overlap [15].

Thin nerve fibers observed in the periosteum are thought to be involved in pain mediation, while thicker fibers may conduct proprioceptive impulses. Since the majority of the periosteal fibers belongs to the former

Correspondence: M. Gajda, Dept. Histology, Jagiellonian University Medical College, Kopernika 7, 31-034 Kraków, Poland;
e-mail: mmgajda@cyf-kr.edu.pl

category, they are considered mainly responsible for nociception. Some reports suggest that bone pain originates predominantly, if not exclusively, from the periosteum [20]. Even pathologies primarily not related to the periosteal lining, such as osteoporosis, osteolytic metastases or inflammatory processes (*osteomyelitis*) are believed to evoke pain sensations from the distorted periosteum.

Although very rich sensory innervation of the periosteum has been demonstrated in many reports, no data is available on the source of sensory innervation to this structure. In the current study we used DiI, a lipophilic axonal tracer, to localize sensory neurons innervating tibial periosteum in rats. DiI was commonly used for *in vivo* and *post mortem* tracing studies of the central and peripheral nervous systems [12, 29, 31] but has not been applied so far on skeleton-related tissues. Additionally, morphometric features discriminating distinct neuronal populations were analyzed by computer-assisted image analysis.

Materials and methods

Animals and surgery. Five male Wistar rats aged 3 months were used for the study. The animals were housed separately in acrylic cages with wood shavings and unlimited access to water and standard rodent food. National and international principles of laboratory animal welfare (conforming to NIH publication nr 86-23, revised 1985) were followed and the experiments were authorized by the local ethics committee. The rats that had been deprived of food overnight were anesthetized by intramuscular injection of fentanyl/fluanizone (Hypnorm®, Janssen, Brussels, Belgium; 0.4 ml/kg b.w.) and treated aseptically throughout the experiment. A longitudinal incision was made through the skin over the proximal portion of the medial surface of the right tibia. The periosteum was exposed and approximately 0.5-2 µl of 2% solution of DiI (1,1'-dioctadecyl-3,3,3',3'-tetramethylindocarbocyanine perchlorate, D-282, Molecular Probes Europe, Leiden, The Netherlands) in methanol was injected *via* a glass micropipette connected to a Pico Spritzer device (Parker Hannifin, USA). The exposed surface was then rinsed with sterile saline and the skin was sutured.

Tissue processing. Four weeks after DiI administration, the animals were deeply anesthetized by an overdose of sodium pentobarbital (Nembutal, Sanofi, Belgium) injected intraperitoneally and transcardially perfused by cold Krebs-Ringer solution followed by 4% buffered (pH=7.4) freshly prepared paraformaldehyde. Dorsal root ganglia of segments Th13, L1-L6 and S1-S4 were dissected bilaterally and immersed in the same fixative overnight at 4°C. The ganglia were then rinsed in PBS and cryoprotected in 25% sucrose in PBS containing 0.01% sodium azide. Serial 14-µm-thick frozen sections were cut along the long axis of each ganglion and mounted on poly-L-lysine-coated slides.

Microscopical analysis. Sections were examined under an Olympus BX50 microscope equipped with a U-MNG filter set (excitation 530-550 nm, emission 590 nm) for visualization of the red fluorescence of DiI. Nucleated fluorescent profiles were counted in all sections. Cell counts were then corrected according to the formula: $N = n[t/(t + d)]$, where N = actual number of neurons, n = number of profiles counted, t = section thickness, d = mean nucleus diameter, to avoid multiple counting of the same perikarya in different sections (modified after [6]). For morphometric analysis, images of the exam-

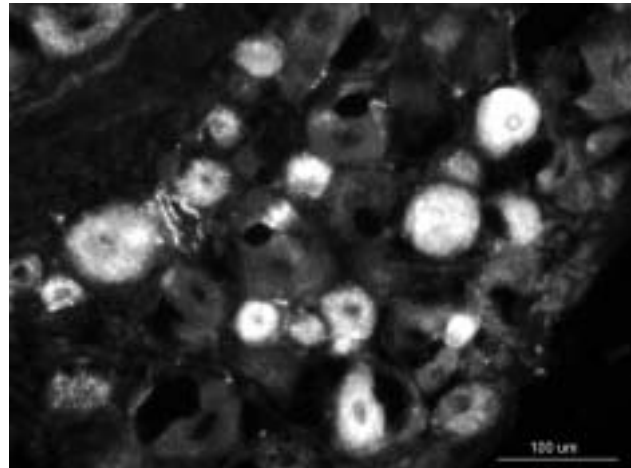


Fig. 1. DiI-labeled perikarya of the L3 dorsal root ganglion.

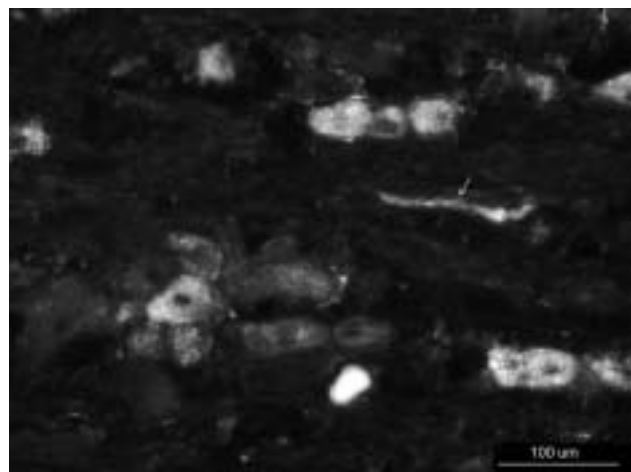


Fig. 2. DiI-labeled perikarya and fiber (arrow) of the L3 dorsal root ganglion.

ined ganglia were acquired using a digital camera (Nikon CoolPix 990) and stored as graphical images (resolution 2048x1536 pixels). Three hundred traced nucleated profiles from different ganglia were registered and measured (area, perimeter, minimal diameter, maximal diameter). The mean diameter was calculated as an average of the maximal and minimal diameter and shape coefficient as a proportion of the minimal diameter to the maximal diameter. The shape coefficient has a value of 1 for circular profiles and decreases as the profile becomes more elongated. The distribution of sizes and shapes of labeled neurons was analyzed and shape coefficients were compared in neuronal populations possessing small and large perikarya. For semiautomatic measurements, the LSM Image Browser 3 software (Zeiss, Germany) was used and statistical analysis was performed using Statgraphics 2.1 for Windows (Manugistics, USA).

Results

Macroscopical analysis of the DiI injection site showed that the tracer was confined to the site of administration and that diffusion to surrounding tissues was negligible.

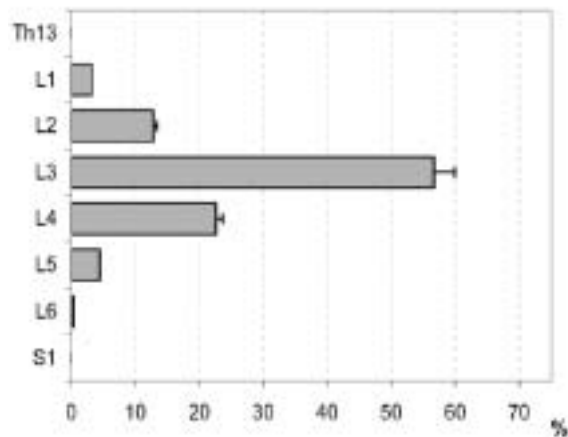


Fig. 3. Segmental distribution of DiI-labeled neurons in dorsal root ganglia. Each bar represents mean \pm SEM (n=5).

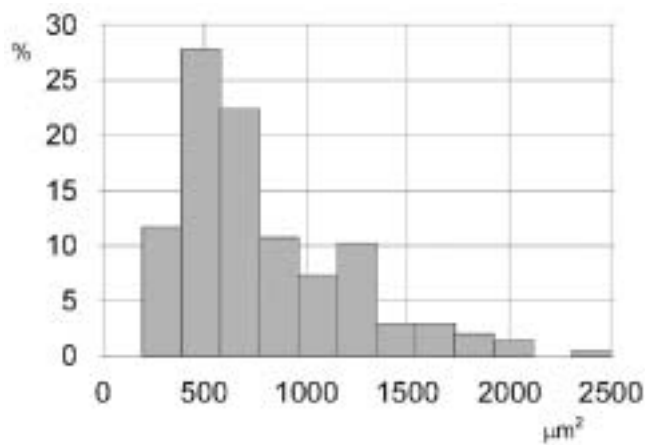


Fig. 4. Size distribution (area) of DiI-labeled neurons in dorsal root ganglia.

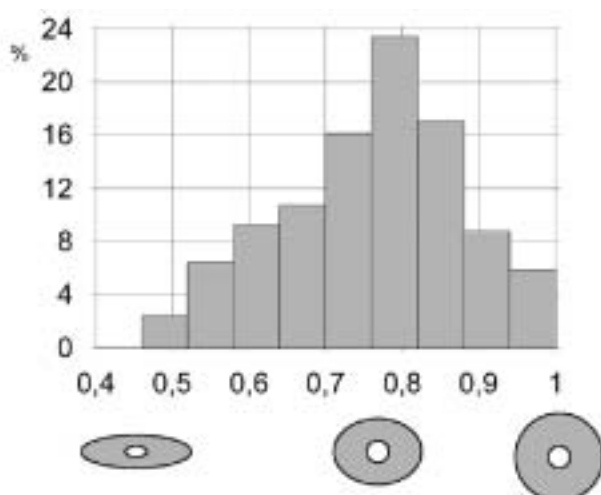


Fig. 5. Shape coefficient distribution of DiI-labeled neurons in dorsal root ganglia. Profiles at the bottom represent respective cell body shapes.

Traced neurons were found in dorsal root ganglia (L1 to L6) and were all located ipsilaterally to the site of tracer administration. Fluorescence intensity varied in different cells. However, DiI-positive neurons - even in case of weak fluorescence - could always be identified unambiguously due to the characteristic granular distribution of the tracer in the perikarya (Figs. 1, 2). Very few DiI-containing nerve fibers were also observed in the examined ganglia (Fig. 2).

The average total number of traced neurons counted in all ganglia per animal amounted to 1530 ± 215 . Most of these neurons (57%) were present in the L3 segment; furthermore, 13% and 23% of labeled neurons were located in L2 and L4 segments, respectively, while the L1 and L5 segments contained sparse and the L6 segment only single perikarya (Fig. 3).

The areas of labeled cell bodies ranged from $270 \mu\text{m}^2$ to $2400 \mu\text{m}^2$ (mean= 782 ± 412), (Fig. 4), the perimeters from $60 \mu\text{m}$ to $180 \mu\text{m}$ (mean= 102 ± 25.8) and the mean diameter from $18 \mu\text{m}$ to $58 \mu\text{m}$ (mean= 39 ± 7.9). The above parameters revealed that the largest population (68% of the traced neurons) consisted of small cells (area $< 850 \mu\text{m}^2$). Medium-sized neurons ($850 \mu\text{m}^2 < \text{area} < 1800 \mu\text{m}^2$) comprised approximately 30% of the labeled population. DiI-labeled perikarya showed a bimodal size distribution with the highest values being $500 \mu\text{m}^2$ and $1300 \mu\text{m}^2$. Large labeled neurons (area $> 1800 \mu\text{m}^2$) were also observed, although their number was very small ($< 2\%$).

Shape coefficient values yielded perikarya of different shape - ranging from nearly spherical to elongated; the most frequently encountered shape was the nearly spherical group with values 0.75-0.95 (Fig. 5). No significant differences ($p=0.28$) in cell body shape were found between the different populations (small, medium-sized and large neurons).

Discussion

DiI, belonging to the class of carbocyanine dyes, is a strongly hydrophobic substance, and hence shows minimal diffusion to the neighbouring tissues and blood vessels. Its presence does not influence vital processes of living cells. DiI has been successfully applied as both antero- and retrograde neuronal tracer in studies of the central and peripheral nervous systems [1, 12, 29]. It is transported by lateral diffusion in the plasma membrane of living neurons at a speed up to 6 mm per day. DiI seems to be a suitable alternative to the commonly used water-soluble tracers, such as Fast Blue and Fluorogold. The absence of dye accumulation in contralateral ganglia confirms that the tracer did not enter the systemic circulation and that there was no nonspecific labeling of other perikarya. The obtained data suggest that DiI can be successfully applied in studies dealing with the innervation sources of bone- and joint-related structures.

Sensory neurons projecting to the tibial periosteum were found in all lumbar dorsal root ganglia of the ipsilateral side, with the majority being present in L3 and L4 segments. This localization corresponds with the origin of sensory fibers running in the rat saphenous nerve (*i.e.*, a branch of the femoral nerve) [3]. This nerve also innervates skin covering medial surfaces of the hindlimb and foot. Our results are in agreement with previous tracing experiments demonstrating sources of sensory and autonomic innervation of the hindlimb. Sensory neurons that were retrogradely traced from the knee joint cavity in rat were located in the L1-L5 segments, with the majority found in the L3 and L4 ganglia [26]. Similar results were obtained in mice [25], although the total number of counted afferents was approximately two times smaller than that observed in rats. Furthermore, injection of Fast Blue into the cartilaginous distal femoral epiphysis in rat pups yielded traced neurons in the ipsilateral spinal ganglia (L2 to L5); 50% of labeled cell bodies were located at L3 level, while 25% and 12% were found at the L4 and L2 levels, respectively [7]. No labeled cells were observed in the L6 ganglion. The present study, however, demonstrates single traced neurons in the L6 ganglion, which may be explained by the more distal localization of the tibial periosteum. A similar distribution of sensory neurons innervating the knee joint was observed in cats, although the majority of the neurons was localized in the L5-L7 ganglia [10]. Nerves and corpuscular receptors located in the crucial ligaments and posterior articular capsule of the knee joint in cats could be identified by anterograde tracing of white germ agglutinin-horseradish peroxidase (WGA-HRP) injected into spinal ganglia at the L5-S1 levels [19]. However, these structures were found to be predominantly innervated by the tibial nerve (*i.e.*, a branch of the sciatic nerve).

The size distribution of perikarya that were retrogradely labeled from the periosteum is similar to the overall size distribution of L5 spinal ganglion neurons of rats [16]; the only exception being a smaller number of large neurons found in the present study. The obtained distribution resembles that of CGRP-immunoreactive neurons from L3 ganglion in the rat [15]. Similar results were also reported in tracing studies of sensory neurons projecting to the cartilaginous distal femoral epiphysis in rat pups, where the vast majority of traced cell bodies was found to belong to the population of small neurons (mean diameter 20-35 μm) [7]. Moreover, 53% of those neurons contained CGRP, 35% were SP-immunoreactive and colocalization of both neuropeptides was found in 33%. Bimodal character was also observed in the size distribution of sensory neurons supplying the prostate gland in cat [6], as well as of CGRP-immunoreactive cells traced from cervical facet joint in rats [23].

The above data justify the suggestion that most of the periosteal afferents of the rat tibia probably contain

CGRP and SP. The CGRP/SP-positive cells are considered primary sensory neurons perceiving pain and temperature and their processes belong to the group of fine, unmyelinated or thin myelinated (C or A δ) fibers. Such fibers are widespread throughout the periosteum covering long bones [4, 13]. Numerous thin and varicose fibers immunoreactive for SP and CGRP are present in the perichondrium/periosteum of long bone rudiments in rats from gestational day 19 onward [11, 27] and they are believed to conduct nociceptive impulses.

The occasional presence (<2%) of large periosteum-projecting sensory neurons is also worth mentioning. Cells of this size had a weakly developed Golgi apparatus, mostly contained neither CGRP nor SP, but were characterized by the presence of a significant amount of neurofilament protein (RT-97 protein) and showed affinity for *Bandeirea simplicifolia* (IB4) lectin [18]. The thick axons of these neurons are mostly myelinated and transmit proprioceptive stimuli. The large DiI-labeled neurons observed in the present study may supply corpuscular receptors (predominantly pacinian corpuscles found in the periosteum [2]).

Acknowledgements: The authors would like to thank Łukasz Szczerba, Katarzyna Pustułka and Ewa Jasek for their excellent technical assistance. The study was supported by grant W1/162/P/L from the Medical College of the Jagiellonian University to M.G.

References

- [1] Adriaensen D, Timmermans JP, Brouns I, Berthoud HR, Neuhuber WL, Scheuermann DW (1998) Pulmonary intraepithelial vagal nodose afferent nerve terminals are confined to neuroepithelial bodies: an anterograde tracing and confocal microscopy study in adult rats. *Cell Tissue Res* 293: 395-405
- [2] Aro H, Eerola E, Aho AJ (1985) Development of nonunions in the rat fibula after removal of periosteal neural mechanoreceptors. *Clin Orthop* 199: 292-299
- [3] Baron R, Janig W, Kollmann W (1988) Sympathetic and afferent somata projecting in hindlimb nerves and the anatomical organization of the lumbar sympathetic nervous system of the rat. *J Comp Neurol* 275: 460-468
- [4] Bjurholm A, Kreicbergs A, Brodin E, Schultzberg M (1988) Substance P- and CGRP-immunoreactive nerves in bone. *Peptides* 9: 165-171
- [5] Bjurholm A, Kreicbergs A, Terenius L, Goldstein M, Schultzberg M (1988) Neuropeptide Y-, tyrosine hydroxylase- and vasoactive intestinal polypeptide-immunoreactive nerves in bone and surrounding tissues. *J Auton Nerv Syst* 25: 119-125
- [6] Danuser H, Springer JP, Katofiasc MA, Thor KB (1997) Extrinsic innervation of the cat prostate gland: a combined tracing and immunohistochemical study. *J Urol* 157: 1018-1024
- [7] Edoff K, Grenegard M, Hildebrand C (2000) Retrograde tracing and neuropeptide immunohistochemistry of sensory neurones projecting to the cartilaginous distal femoral epiphysis of young rats. *Cell Tissue Res* 299: 193-200
- [8] Gajda M, Adriaensen D, Cichocki T (2000) Development of the innervation of long bones: expression of the growth-associated protein 43. *Folia Histochem Cytobiol* 38: 103-110
- [9] Gronblad M, Liesi P, Korkala O, Karaharju E, Polak J (1984) Innervation of human bone periosteum by peptidergic nerves. *Anat Rec* 209: 297-299

- [10] Hanesch U, Heppelmann B (1995) A simple method for a specific retrograde labelling of dorsal root and sympathetic ganglion cells innervating the knee joint of the cat. *J Neurosci Methods* 63: 55-59
- [11] Hara-Irie F, Amizuka N, Ozawa H (1996) Immunohistochemical and ultrastructural localization of CGRP-positive nerve fibers at the epiphyseal trabecules facing the growth plate of rat femurs. *Bone* 18: 29-39
- [12] Hens J, Gajda M, Scheuermann DW, Adriaensen D, Timmermans JP (2002) The longitudinal smooth muscle layer of the pig small intestine is innervated by both myenteric and submucous neurons. *Histochem Cell Biol* 117: 481-492
- [13] Hill EL, Elde R (1991) Distribution of CGRP-, VIP-, D β H-, SP-, and NPY-immunoreactive nerves in the periosteum of the rat. *Cell Tissue Res* 264: 469-480
- [14] Hill EL, Turner R, Elde R (1991) Effects of neonatal sympathectomy and capsaicin treatment on bone remodeling in rats. *Neuroscience* 44: 747-755
- [15] Ju G, Hokfelt T, Brodin E, Fahrenkrug J, Fischer JA, Frey P, Elde RP, Brown JC (1987) Primary sensory neurons of the rat showing calcitonin gene-related peptide immunoreactivity and their relation to substance P-, somatostatin-, galanin-, vasoactive intestinal polypeptide- and cholecystokinin-immunoreactive ganglion cells. *Cell Tissue Res* 247: 417-431
- [16] Kishi M, Tanabe J, Schmelzer JD, Low PA (2002) Morphometry of dorsal root ganglion in chronic experimental diabetic neuropathy. *Diabetes* 51: 819-824
- [17] Levine JD, Clark R, Devor M, Helms C, Moskowitz MA, Basbaum AI (1984) Intra-neuronal substance P contributes to the severity of experimental arthritis. *Science* 226: 547-549
- [18] Mach DB, Rogers SD, Sabino MC, Luger NM, Schwei MJ, Pomonis JD, Keyser CP, Clohisy DR, Adams DJ, O'Leary P, Mantyh PW (2002) Origins of skeletal pain: sensory and sympathetic innervation of the mouse femur. *Neuroscience* 113: 155-166
- [19] Madey SM, Cole KJ, Brand RA (1997) Sensory innervation of the cat knee articular capsule and cruciate ligament visualised using anterogradely transported wheat germ agglutinin-horseradish peroxidase. *J Anat* 190: 289-297
- [20] Mercadante S (1997) Malignant bone pain: pathophysiology and treatment. *Pain* 69: 1-18
- [21] Miller MR, Kasahara M (1963) Observations on the innervation of human long bones. *Anat Rec* 145: 13-23
- [22] Nagy JI, Iversen LL, Goedert M, Chapman D, Hunt SP (1983) Dose-dependent effects of capsaicin on primary sensory neurons in the neonatal rat. *J Neurosci* 3: 399-406
- [23] Ohtori S, Moriya H, Takahashi K (2002) Calcitonin gene-related peptide immunoreactive sensory DRG neurons innervating the cervical facet joints in rats. *J Orthop Sci* 7: 258-261
- [24] Ralston HJ, Miller MR, Kasahara M (1960) Nerve endings in human fascia, tendons, ligaments, periosteum, and joint synovial membrane. *Anat Rec* 136: 137-147
- [25] Salo PT, Tatton WG (1993) Age-related loss of knee joint afferents in mice. *J Neurosci Res* 35: 664-677
- [26] Salo PT, Theriault E (1997) Number, distribution and neuropeptide content of rat knee joint afferents. *J Anat* 190: 515-522
- [27] Sisask G, Bjurholm A, Ahmed M, Kreicbergs A (1995) Ontogeny of sensory nerves in the developing skeleton. *Anat Rec* 243: 234-240
- [28] Skofitsch G, Jacobowitz DM (1985) Calcitonin gene-related peptide coexists with substance P in capsaicin sensitive neurons and sensory ganglia of the rat. *Peptides* 6: 747-754
- [29] Song A, Ashwell KW, Tracey DJ (2000) Development of the rat phrenic nucleus and its connections with brainstem respiratory nuclei. *Anat Embryol* 202: 159-177
- [30] Thurston TJ (1982) Distribution of nerves in long bones as shown by silver impregnation. *J Anat* 134: 719-728
- [31] von Bartheld CS, Cunningham DE, Rubel EW (1990) Neuronal tracing with DiI: decalcification, cryosectioning, and photoconversion for light and electron microscopic analysis. *J Histochem Cytochem* 38: 725-733

Accepted January 12, 2004